An EOF Iteration Approach for Obtaining Homogeneous Radiative Fluxes from Satellites Observations

Banglin Zhang (1), Rachel T. Pinker (2) and Paul W. Stackhouse, Jr. (3)

(1) Global Modeling and Assimilation Office, Code 610.1

SAIC, Goddard Space Flight Center Greenbelt, MD 20771

(2) Department of Meteorology

University of Maryland, College Park, MD 20742

(2) NASA Langley Research Center

21 Langley Boulevard, Mail Stop 420

Hampton, VA 23681-2199

Submitted to Journal of Applied Meteorology

September 4, 2005

Revised version:

May 2006

Final Version

August 2006

Corresponding Author:

Rachel T. Pinker

University of Maryland

Department of Atmospheric and Oceanic Science

College Park, MD 20742

pinker@atmos.umd.edu Tel: 301-405-5380 FAX: 301-314-9482

Abstract

Conventional observations of climate parameters are sparse in space and/or in time and the representativeness of such information needs to be optimized. Observations from satellites provide improved spatial coverage than point observations however they pose new challenges for obtaining homogeneous coverage. Surface radiative fluxes, the forcing functions of the hydrologic cycle and biogeophysical processes, are now becoming available from global scale satellite observations. They are derived from independent satellite platforms and sensors that differ in temporal and spatial resolution and in the size of the footprint from which information is derived. Data gaps, degraded spatial resolution near boundaries of geostationary satellites, and different viewing geometries in areas of satellite overlap, could result in biased estimates of radiative fluxes. In this study, discussed will be issues related to the sources of inhomogeneity in surface radiative fluxes as derived from satellites; development of an approach to obtain homogeneous data sets; and application of the methodology to the widely used International Satellite Cloud Climatology Project (ISCCP) data that currently serve as a source of information for deriving estimates of surface and top of the atmosphere radiative fluxes. Introduced is an Empirical Orthogonal Function (EOF) iteration scheme for homogenizing the fluxes. The scheme is evaluated in several ways including comparison of the inferred radiative fluxes against ground observations, both before and after the EOF approach is applied. On the average, the latter reduces the rms error by about 2-3 W/m^2.

1. Introduction

1.1 At issue

To advance the understanding of the water cycle and land-atmosphere interactions on global scale, information on radiative fluxes is needed at similar scales, and in principle, can be obtained from satellite observations. Only recently global scale satellite observations at climatic time scales have become available. While issues related to paucity of data have been addressed in the past, each climatic parameter poses a unique challenge for obtaining homogeneous time series representative of large spatial scales. The most widely used parameter to study climate variability is surface temperature, either at shelter level over land stations, or sea surface temperature (SST), as derived both from satellites and in-situ observations. Reynolds and Smith (1995) developed an optimal interpolation (OI) technique implemented weekly at 1^0 resolution using ship and buoy data of SST and satellite data. In their approach attention is given to the removal of large-scale biases of satellite data, as compared to in situ data. Smith et al. (1996) expanded this approach by using the best estimates of the full covariance structure of the mean SST fields to fit the in situ data and fill data gaps. They used spatial functions defined by empirical orthogonal functions (EOF), computed from a principal component analysis (PCA). It is claimed that this approach is an improvement over the OI method, which utilized local interpolation with modeled covariance functions, while in the newer scheme basin wide covariance structures are used. Other studies dealt with various aspects of interpolation needs of climatic parameters, emphasizing different aspects of the problem. For example, Rayner et al. (1995) attempt to improve global long term sea ice and SST analysis while Shriver and O'Brien (1995) address the wind stress issue. Radiative fluxes as derived from satellites

are more recent climate parameters that are becoming available at spatial and temporal scales of interest in climate research. These pose a different type of difficulties than those addressed previously, and will be addressed in this study.

1.2 Satellite data to be used

The International Satellite Cloud Climatology Project is a major program of the World Climate Research Program (WCRP) for preparing satellite observations, which are suitable for inferring global distribution of clouds, their properties, and their effect on the radiation balance (Schiffer and Rossow, 1983; Schiffer and Rossow, 1985; Rossow and Schiffer, 1991; Rossow and Garder, 1993a and 1993b; Brest et al., 1997; Rossow and Schiffer, 1999). Data collection began on July 1, 1983, continued through 2006 and there are plans for extension beyond 2006.

The ISCCP D1 data are at 2.5 degree spatial resolution and 3-hourly time intervals. They are based on observations made from several geostationary and polar orbiting satellites. These data have been extensively used for inferring global scale distributions of clouds, cloud properties, and surface radiative fluxes (Han et al. 1995; Zhang et al. 1995; Pinker and Laszlo, 1992; Tselioudis et al. 2000; Zhang et al. 2004; Pinker et al. 2005). Geophysical parameters derived from the ISCCP D1 data have also been used in a wide range of applications (Hahmann et al., 1995; Bony et al. 1997; Machado et al. 1998; Prigent et al. 1998; Sui et al. 2003). For studies of the hydrologic cycle at regional scale, information on surface radiative fluxes is needed at high spatial resolution. The ISCCP DX satellite observations (the basis for the D1 data-set) are made at 30 km resolution from several geostationary and polar orbiting satellites as provided by various agencies. The

Tiros-N data come from the National Oceanic and Atmospheric Administration (NOAA); the METEOSAT data are provided by the European Meteorological Satellite Organization (EUMETSAT); the GOES-EAST data are provided by the Meteorological Service of Canada; the GOES-WEST data come from the University of Colorado, Cooperative Institute for Research in the Atmosphere (CIRA); and the GMS data come from the Japan Meteorological Agency. The observations are not homogeneous in terms of spatial and temporal coverage; in particular, when geostationary satellites are used, merging issues arise.

1.2.1 Motivation for study

Data from geostationary satellites at the ISCCP DX level are provided independently for each satellite. An ISCCP DX product is also available from polar orbiting satellites, and is provided on an orbit-by-orbit basis, covering the entire globe. When all available observations at the DX level are combined from all the observing platforms, the coverage density is as presented in **Figure 1 (a)**. At any particular time and location, climatic information inferred from these observations will be affected by the uneven distribution of the observations. The objective of this study is to develop an approach for optimal smoothing and interpolation of the derived surface radiative fluxes as obtained from the raw satellite observations. Discussion will focus on the surface short-wave radiative fluxes derived from the ISCCP DX data from GOES and METEOSAT satellites only, since in these regions ample ground observations are available for the evaluation of the methodology.

1.2.2 Methodology to derive surface radiative fluxes

The primary objective of this study is to develop a methodology that will provide homogeneous information on surface and top of the atmosphere radiative fluxes for large areas. For estimating the surface short-wave (SW), Photosynthetically Active Radiation (PAR), and near-infrared (NIR) fluxes from the satellite observations at both boundaries of the atmosphere from the ISCCP DX data, an inference technique developed at the University of Maryland (Pinker and Laszlo 1992) is used. The method is based on radiative transfer theory, and produces direct and diffuse fluxes in five spectral intervals in the 0.2-4.0 μm range. The radiative transfer model accounts for the absorption and scattering processes occurring in the atmosphere and for the interaction of the radiation with the surface. The interaction with the surface is modeled spectrally, and allows incorporation of spectral observations that are becoming available from EOS observations (MODerate resolution Imaging Spectrometer (MODIS) (King et al., 1992) and the Global Imager (GLI) sensor, on the Advanced Earth Observing Satellite (ADEOS-II)).

The radiative fluxes at the boundaries of the atmosphere are computed by determining atmospheric transmission and reflection (optical functions) and the surface albedo, pertaining to a particular satellite observation. The retrieved optical functions, along with the surface albedos, are then used to independently compute the fluxes for clear and cloudy conditions. The all-sky flux is obtained by using information on cloud cover. The fluxes for this study were produced at the University of Maryland with Version 2.1 of the Global Energy and Water cycle EXperiment/Surface Radiation Budget (UMD/SRB) model (Whitlock et al. 1995; Pinker et al. 1995), which includes improved

parameterization of water vapor absorption (Ramaswamy and Freidenreich, 1992) as well as improved techniques for replacing missing observations as compared to Version 1.1. Missing values were replaced based on time-space interpolation. This latter version has been implemented at the Surface Radiation Budget/Satellite Data Analysis center (SDAC) at NASA Langley Research Center with ISCCP C1 data at 2.5 degree resolution for July 1983-December 1988, and results are available from the Langley DAAC at: http://eosweb.larc.nasa.gov/. More recently, it is being implemented at LaRC at 1 degree resolution and results are available at: http://srb-swlw.larc.nasa.gov/GEWEX_SRB_homepage.html

The monthly mean shortwave downward flux (W/m^2) for January 1992 as derived from ISCCP DX data from GOES, METEOSAT, and GMS is illustrated in **Figure 2** (b). To obtain homogeneous and coherent radiative fluxes from the satellite observations requires addressing issues related to uneven sampling, data gaps, degraded spatial resolution as one moves away from the nadir, and different viewing geometries in areas of overlap. The Empirical Orthogonal Function **(**EOF) iteration scheme is well suited for getting integrated, smoothed, high-resolution surface radiative fluxes, because in this approach, spatial modes are derived statistically from available observations and then used to reconstruct the information in areas of degraded data quality. It should be pointed out that the ISCCP data are normalized to one reference polar orbiting satellite (afternoon) measurements and in addition, the residuals from the normalization are further corrected by calibration adjustment, so that certain inhomogeneity/incoherence in the ISCCP DX data are removed to begin with. Selected available interpolation methodologies and the one used in this study will be presented in Section 2. Evaluation

of the proposed methodology will be discussed in Section 3. Conclusions and discussion will be presented in Section 4.

2. Interpolation schemes

2.1 Available methodologies

For data gap filling and interpolation, several schemes have been developed. For example, Renka (1997a, 1997b) developed an interpolation approach using piecewise linear interpolation functions. Optimal interpolation (OI) techniques are more widely used for meteorological applications (Lorenc, 1981). OI is performed locally with modeled covariance functions that take into account local data structure. The interpolated fields from both OI and simple interpolation schemes are usually used for relatively small regions and can result in isolated anomalies due to unreasonable stretching of data to fill the gaps.

Smith et al. (1996) developed an interpolation method using EOFs from OI analyses to remove deficiencies in SST interpolated fields. The core of the method is based on the adaptation of EOF reconstruction techniques used to fill gaps in the gridded data-sets. The approach involves (i) development of spatial EOFs from recent data-rich years; (ii) use of dominant EOF modes as basis functions that are fitted to available data from earlier data-poor years; and (iii) reconstruction of global SST fields from these spatial and temporal modes. The EOFs efficiently use the best estimate of the full covariance structure of the monthly mean SST fields to fit in situ SST observations to data voids and field smoothing. This method can be used to interpolate other atmospheric and oceanograghic data.

2.2 *Empirical Orthogonal Function (EOF) iteration scheme*

When applied to satellite estimates of radiative fluxes that have both missing and degraded data, the Smith et al. EOF reconstruction scheme can not distinguish between good and degraded quality observations. This problem can be addressed by using an EOF iteration approach. The scheme was first developed by Zhang et al (1993) to forecast multi-dimensional time series and was applied to ENSO prediction (Zhang and Pan, 1996). Before applying the EOF iteration scheme for interpolation and gap filling, the data are first divided into two groups: a) high quality, such as observations near nadir where the frequency of observations is high (anchor region); b) lower quality, such as the regions near viewing edges of each satellite; regions of overlap with different viewing geometry; and regions where data are missing. In **Figure 2** illustrated are two examples of possible selection of anchor regions for ISCCP DX GOES and METOSAT satellites. In order to derive a "first guess" field for the EOF analysis, used is Version 2.1 of UMD/SRB model to process at daily time scale the ISCCP DX data from METEOSAT and GOES satellite for the period 1989-1993 at 0.5-degree resolution to derive the daily radiative fluxes. For each month, the daily fluxes in areas of overlap are averaged and missing data are replaced with fluxes derived from the ISCCP D1 data, interpolated to 0.5-degree spatial resolution, using the interpolation approach developed by Renka (1997a, 1997b). These data serve as a first guess in the iteration process. We create a data matrix, which consists of the departures of the "first guess" field from the monthly mean, in the form:

$$F^{(0)}_{NxM} = \begin{bmatrix} f^{(0)}_{11} & f^{(0)}_{12} & \cdots & f^{(0)}_{1M} \\ f^{(0)}_{21} & f^{(0)}_{22} & \cdots & f^{(0)}_{2M} \\ \cdots & \cdots & \cdots & \cdots \\ f^{(0)}_{N1} & f^{(0)}_{N2} & \cdots & f^{(0)}_{NM} \end{bmatrix} \qquad (1)$$

where N is the number of time series (for example, it is 31 daily average values of surface short-wave flux deviations from the January monthly mean), and M is the number of all spatial grids for the data set.

The EOF analysis is applied on the data matrix $F^{(0)}$ to produce eigenvalues in a descending order (from larger to smaller ones) and associated EOF modes. The first EOF accounts for most of the total variance. Each following EOF explains a smaller part of the total variance. The ratio between the accumulated eigenvalues of the first K EOFs and the sum of all eigenvalues represents the percentage variance explained and is often the basis for deciding what should be the number of EOFs to retain. For example, in **Figure 3**, illustrated is the explained variance as a function of the number of EOF modes used for January and July of 1992. We use the ratio of 80% to select the number of EOF modes which explain 80% of the total variance of the first guess field. In this case, twenty EOFs will explain about 80 % of the total variance. Therefore, the first twenty EOFs are selected to reconstruct the data in the first iteration step. Subsequently, the EOF analysis is repeated using the available data in the high quality regions (the "anchor" regions), and the reconstructed data in the poor quality region. The resulting "fusing" scheme will iteratively replace the data in the degraded domain by propagating

information from the high quality regions. It should be pointed out that the EOF iteration scheme does not address problems that may be caused by biases between different instruments.

The initial reconstructed field is obtained as follows:

$$\hat{F}^{(0)}_{NxM} = \sum_{k=1}^{K_0^{(0)}} Y_k^{(0)} X_k^{(0)} = \begin{bmatrix} \hat{f}^{(0)}_{11} & \hat{f}^{(0)}_{12} & \cdots & \hat{f}^{(0)}_{1M} \\ \hat{f}^{(0)}_{21} & \hat{f}^{(0)}_{22} & \cdots & \hat{f}^{(0)}_{2M} \\ \cdots & \cdots & \cdots & \cdots \\ \hat{f}^{(0)}_{N1} & \hat{f}^{(0)}_{N2} & \cdots & \hat{f}^{(0)}_{NM} \end{bmatrix} \quad (2)$$

Here $Y_k^{(0)}$ and $X_k^{(0)}$ are the principal components and EOF modes derived from the first guess $F^{(0)}_{NxM}$. Subsequently, the missing values and degraded data are replaced with the corresponding values in $\hat{F}^{(0)}_{NxM}$, and a new matrix $F^{(1)}_{NxM}$ is created. Now the EOF analysis is performed on $F^{(1)}_{NxM}$, and the following new reconstructed field is obtained:

$$\hat{F}^{(1)}_{NxM} = \sum_{k=1}^{K_0^{(1)}} Y_k^{(1)} X_k^{(1)} = \begin{bmatrix} \hat{f}^{(1)}_{11} & \hat{f}^{(1)}_{12} & \cdots & \hat{f}^{(1)}_{1M} \\ \hat{f}^{(1)}_{21} & \hat{f}^{(1)}_{22} & \cdots & \hat{f}^{(1)}_{2M} \\ \cdots & \cdots & \cdots & \cdots \\ \hat{f}^{(1)}_{N1} & \hat{f}^{(1)}_{N2} & \cdots & \hat{f}^{(1)}_{NM} \end{bmatrix} \quad (3)$$

This reconstructed field is then used to replace the missing and degraded values to create $F^{(2)}_{NxM}$ for next EOF analysis. Iteratively, the EOF analysis is repeated up to the nth step, the degraded data and missing values are replaced each time until the process converges.

In the final step, EOF smoothing is applied on the entire data set, including the "anchor" regions, resulting in the final reconstructed and smoothed field given as:

$$\hat{F}^{(n)}_{NxM} = \sum_{k=1}^{K_0^{(n)}} Y_k^{(n)} X_k^{(n)} = \begin{bmatrix} \hat{f}^{(n)}_{11} & \hat{f}^{(n)}_{12} & \cdots & \hat{f}^{(n)}_{1M} \\ \hat{f}^{(n)}_{21} & \hat{f}^{(n)}_{22} & \cdots & \hat{f}^{(n)}_{2M} \\ \cdots & \cdots & \cdots & \cdots \\ \hat{f}^{(n)}_{N1} & \hat{f}^{(n)}_{N2} & \cdots & \hat{f}^{(n)}_{NM} \end{bmatrix} \qquad (4)$$

In **Figure 4**, the convergence process is illustrated for January and July of 1992. The RMS difference for the entire field between successive iteration steps is calculated, normalized by the standard deviation. When this difference is less than 0.5 %, the iteration process is complete. **Figure 4** shows that about 7-8 iterations are needed for converge. The final filled values are the sum of the base monthly mean and the interpolated values from the EOF iteration scheme.

3. Evaluation of the merging process

3.1 Qualitative evaluation

The EOF iteration scheme was applied to surface shortwave radiation derived from METEOSAT and GOES at daily time scale for January 1992, over (70^0 S -70^0 N, 180^0 W-70^0 E). Illustrated are the results for the two control tests. In the first test, the sub-region 20^0 S-20^0 N, 130^0-70^0 W where observations are most dense is chosen as a test region, and the computed fluxes are removed for the entire month from all grids except for 5 by 5 grids. For the artificially missing values, the Renka scheme is used to get a first guess, and subsequently, the EOF scheme is run with and without the iteration approach (without the iteration it is equivalent to the Smith method). The daily

shortwave downward fluxes on January 2, 1992 are shown in **Figure 5 (a)** for actual observations, as estimated by the Renka interpolation scheme, the Smith EOF reconstruction scheme, and EOF iteration scheme. No significant difference is observed for the three schemes. The RMS differences between actual daily values and estimations are 30.13, 27.19, and 27.43 Wm^{-2} for Renka scheme, Smith scheme, and EOF iteration scheme, respectively.

In the second control test, data are removed from the entire sub-region 20 S-20 N, 130-70 W on even days for the month of January 1992 **Figure 5 (b)** shows the original field before removing data for the tests and estimates from the three interpolation schemes on January 2, 1992. As seen, the results from all 3 interpolation schemes have degraded when compared with the control test. However, results from the EOF iteration scheme are smoother than the results from the Renka or Smith schemes. The RMS differences between the original daily values and estimates are 53.66, 49.74, and 47.36 Wm^{-2} for the Renka, Smith, and EOF iteration schemes, respectively. Based on both spatial structure and RMS differences, the EOF iteration scheme seems to perform better than the Renka and Smith schemes.

Sensitivity tests were conducted by using two possible ways to select "anchor" regions and regions of degraded information as illustrated in **Figure 2** for January 1992. It was shown that the differences in the derived fluxes using the different anchor regions were quite small. This was repeated for July 1992 and again, the differences in the derived fluxes were small.

3.1 Quanitative evaluation

A quantitative evaluation of the impact of the proposed merging methodology on the derived surface fluxes was performed by comparison of results from Renka scheme, Smith method, and EOF iteration scheme against ground observations on a daily time scale. For this purpose, used was a partial archive of ground truth as available at the NASA Langley Research Center and as described in Chiacchio et al. (2004). The broadband SW surface measurements were provided by the World Radiation Data Center (WRDC/GEBA)/Canadian Networks. Chosen were sites with continuous long-term observations in regions observed by the two geostationary satellites GOES and METEOSAT. Used was the period 1989 to 1993 for which the proposed methodology has been implemented. The sites used in this study are shown in **Figure 6.** The analysis was done separately for North America and for Africa. Used were all available stations for each region which resulted in 9447 data points for North America and 59796 data points for Africa; independent statistics were performed for several sub-regions clustered by proximity to each other, as show in Figure 8. The complete statistics for each sub-region as well as for North America and for Africa is presented in **Table 1.** As evident**,** when comparing Renka method, the Smith method and EOF iteration scheme reduced the average rms was reduced by about 2-3 Wm^{-2} while the bias was reduced by about 5-6 Wm^{-2}. The bias and rms averages from EOF iteration are slightly smaller than from the Smith method. It is believed that in regions of highly degraded observations or sparse coverage, the improvements would be better. Due to the sparcity of observations in such regions it was not possible to undertake such specific analysis at this time. Illustration of

results for all N. America using all ground observations and for Africa, using observations in region III only, is given in **Figure 7.**

4. Discussion

The inhomogeneity of satellite observations used in the evaluation of estimated surface parameters (e.g., surface radiation or surface temperature) against ground observations will impact the demonstrated accuracy. Similar problems arise when satellite estimates are used to evaluate climate or numerical weather prediction models, which have homogeneous grids. Therefore, it is important to 'homogenize' the various satellite-based parameters in a way that the effect of inhomogeneity and incoherence will be minimized. In the present study, an effort in that direction has been made. Specifically, an EOF analysis was used to utilize observations in regions of frequent observations, to propagate temporal and spatial structural information into regions of missing or degraded observations. It was demonstrated that this approach resulted in improved estimates of surface fluxes as well as in smoothed and coherent fields.

Acknowledgement

This work was initiated under grant NAGW4740 from the Earth Science Data and Information Branch and continued under grant NAG56667 from the Mission to Planet Earth (MTPE) Program, Science Division. The ISCCP data were obtained from the NASA Langley Research Center EOSDIS Distributed Active Archive Center.

References:

Bony S, Y. Sud, K. M. Lau, J. Susskind, and S. Saha, 1997: Comparison and satellite assessment of NASA/DAO and NCEP-NCAR reanalysis over tropical oceans: Atmospheric hydrology and radiation. *J. Climate,* **10 (6),** 1441-1462.

Brest, C. L., W. B. Rossow, and M. Roiter, 1997: Update of Radiance Calibrations for ISCCP. *J. Atmos. Ocean Tech.,* **14,** 1091-1109.

Chiacchio, M., P. W. Stackhouse Jr., S. K. Gupta, S. J. Cox, J. C. Mikovitz, paper presented at the American Geophysical Union 2004 Spring Meeting, Montreal, Quebec, Canada, 2004.

Han Q., W. B. Rossow, R. Welch, A. White, and J. Chou, 1995: Validation of satellite retrievals of cloud microphysics and liquid water path using observations from FIRE. *J. Atmos. Sci.,* **52** (23), 4183-4195.

Hahmann, A. N., Ward, D. M., and Dickinson, R. E., 1995: Land-surface temperature and radiative fluxes response of the NCAR CCM2 Biosphere-Atmosphere Transfer Schemes to modifications in the properties of clouds. *J. Geophys. Res.-Atmos*, **100 (D11),** 23239-23252.

King, M. D., Y. J. Kaufman, W. P. Menzel, and D. Tanré, 1992: Remote sensing of cloud, aerosol, and water vapor properties from the Moderate Resolution Imaging Spectrometer (MODIS). *IEEE Transactions on Geosciences and Remote Sensing*, **30**, 2-27.

Lorenc, A., 1981: A global three-dimensional multivariate statistical interpolation scheme. *Mon. Wea. Rev.* **109**, 701-721.

Machado L. A. T., W. B. Rossow, R. L. Guedes, and A. W. Walker, 1998: Life cycle variations of mesoscale convective systems over the Americas. *Mon. Weather Rev.*, **126 (6),** 1630-1654.

Pinker, R. T., I. Laszlo, C. H. Whitlock, and T. P. Charlock, 1995: Radiative Flux Opens New Window on Climate Research. *EOS*, **76**, No. 15, April 11.

Pinker, R. T. and I. Laszlo, 1992: Modeling of surface solar irradiance for satellite applications on a global scale. *J. Appl. Meteor.*, **31**, 194-211.

Pinker, R. T., B. Zhang, and E. G. Dutton, 2005: Do Satellites Detect Trends in Surface Solar Radiation?. Science 308: 850-854.

Prigent C., W. B. Rossow, and E. Matthews, 1998: Global maps of microwave land surface emissivities: Potential for land surface characterization. *Radio Sci*., **33 (3),** 745-751.

Ramaswamy, V., and S. M. Freidenreich, 1992: A study of broadband parameterizations of the solar radiative interactions with water vapor and water drops. *J. Geophys. Res.*, **97**, 11,487-11,512.

Rayner, N. A., C. K. Folland, D. E. Parker, and E. B. Horton, 1995: A new global sea-ice and sea surface temperature (GISST) data set for 1903\x{2013}1994 for forcing climate models. Hadley Centre Internal Note 69, 13 pp.

Renka, R. J., 1997a: ALGORITHM 772. STRIPACK: Delaunay Triangulation and Voronoi Diagram on the surface of a sphere, ACM Trans. Math. Software 23, No.3, Sept. 1997, pp.415-434.

Renka, R. J., 1997b: ALGORITHM 773. SSRFPACK: Interpolation of scattered data on the surface of a sphere with a surface under tension, ACM Trans. Math. Software 23, No.3, Sept. 1997, pp. 435-442.

Reynolds, R. W., and T. M. Smith, 1995: A high resolution global sea surface temperature climatology. *J. Climate*, **8,** 1571-1583.

Rossow, W. B., A. Walker, and M. Roiter, 1996: Revision: International Satellite Cloud Climatology Project (ISCCP) Description of Reduced Resolution Radiance Data. *WMO/TD-No.* **58**. World Meteorological Organization, 163 pp.

Rossow, W. B., and L. C. Garder, 1993a: Cloud detection using satellite measurements of infrared and visible radiances for ISCCP. *J. Climate*, **6**, 2370-2393.

Rossow, W. B., and L. C. Garder, 1993b: Validation of ISCCP cloud detections. *J. Climate*, **6,** 2370- 2393.

Rossow, W. B., and R. A. Schiffer, 1991: ISCCP Cloud Data Products. *Bull. Amer. Meteor. Soc*., **71**, 2-20.

Rossow, W. B., and R. A. Schiffer, 1999: Advances in Understanding Clouds from ISCCP. *Bull. Amer. Meteor. Soc*., **80,** 2261-2287.

Schiffer, R. A., and Rossow, W. B., 1983: The International Satellite Cloud Climatology Project (ISCCP): The First Project of the World Climate Research Programme. Bull. *Amer. Meteor. Soc*., **64**, 779-784.

Schiffer, R. A., and Rossow, W. B., 1985: ISCCP Global Radiance Data Set: A New Resource for Climate Research. *Bull. Amer. Meteor. Soc*., 66, 1498-1505.

Shriver, Jay F., and J. J. O'Brien, 1995: Low-frequency Variability of the Equatorial Pacific Ocean Using a New Pseudostress Dataset: 1930-1989. J. of Climate, **8**, 2762-2786.

Smith, T. M., R. W. Reynolds, R. E. Livezey, and D. C. Stokes, 1996: Reconstruction of historical sea surface temperatures using empirical orthogonal functions. *J. Climate,* **9,** 1403-1420.

Sui, C.-H., W. K.-M. Lau, X. Li, M. M. Rienecker, I. Laszlo, and R. T. Pinker, 2003: The Impacts of Daily Surface Forcing in the upper Ocean over tropical Pacific: A Numerical Study. *J. Climate*, 16 (4), 756-766.

Tselioudis, G., Y. C. Zhang, and W. B. Rossow, 2000: Cloud and radiation variations associated with northern midlatitude low and high seal level pressure regimes. *J. Climate*, **13 (2),** 312-327.

Whitlock, C. H., T. P. Charlock, W. F. Staylor, R. T. Pinker, I. Laszlo, A. Ohmura, H. Gilgen, T. Konzelman, R. C. DiPasquale, C. D. Moats, S. R. LeCroy, and N. A. Ritchey, 1995: First Global WCRP Short-wave surface Radiation Budget Data Set. *Bull. Amer. Meteor. Soc.* **76**, No. 6, 1-18.

Zhang, B., J. Liu, and Z. Sun, 1993: A new multidimensional time series forecasting method based on EOF iteration scheme. *Advances in Atmospheric Sciences, Vol. 10,* pp. 243-247.

Zhang, B. and J. Pan, 1996: Forecasts of tropical Pacific SST anomalies using a statistical (EOF) iteration model, Experimental Long-Lead Forecast *Bull.*, **5**, No. *2*, pp. 60-62.

Zhang Y. C., W. B. Rossow, and A. A. Lacis, 1995: Calculation of surface and top of the atmosphere radiative fluxes from physical quantities based on ISCCP data sets. 1. Method and Sensitivity to input data uncertainties. *J. Geophys. Res-Atmos*, **100** (D1), 1149-1165.

Zhang Y. C., W. B. Rossow, A. A. Lacis, V. Oinas, and M. I. Mishchenko, 2004: Calculation of radiative fluxes from the surface to top of atmosphere based on ISCCP and other global data sets: Refinements of the radiative transfer model and the input data. *J. Geophys. Res-Atmos*, **109,** D19105.

List of Figures

Figure 6. Location of stations used for evaluation of the improvements in surface radiative fluxes as a result of the proposed merging procedure. Circle: North America Region 1 (NA1); oentagram: North America Region 2 (NA2); hexagram: Africa Region 1 (AF1); asterick: Africa Region 2 (AF2); square: Africa Region 3 (AF3); and diamond: Africa Region 4 (AF4).

Figure 7. Comparison of merged surface SW radiative fluxes as derived from ISCCP DX data gridded to 0.5^0 against ground observations for the period 1989-1993. Over North America, results are illustrated for all available stations. Over Africa, results are illustrated only for stations in region III.

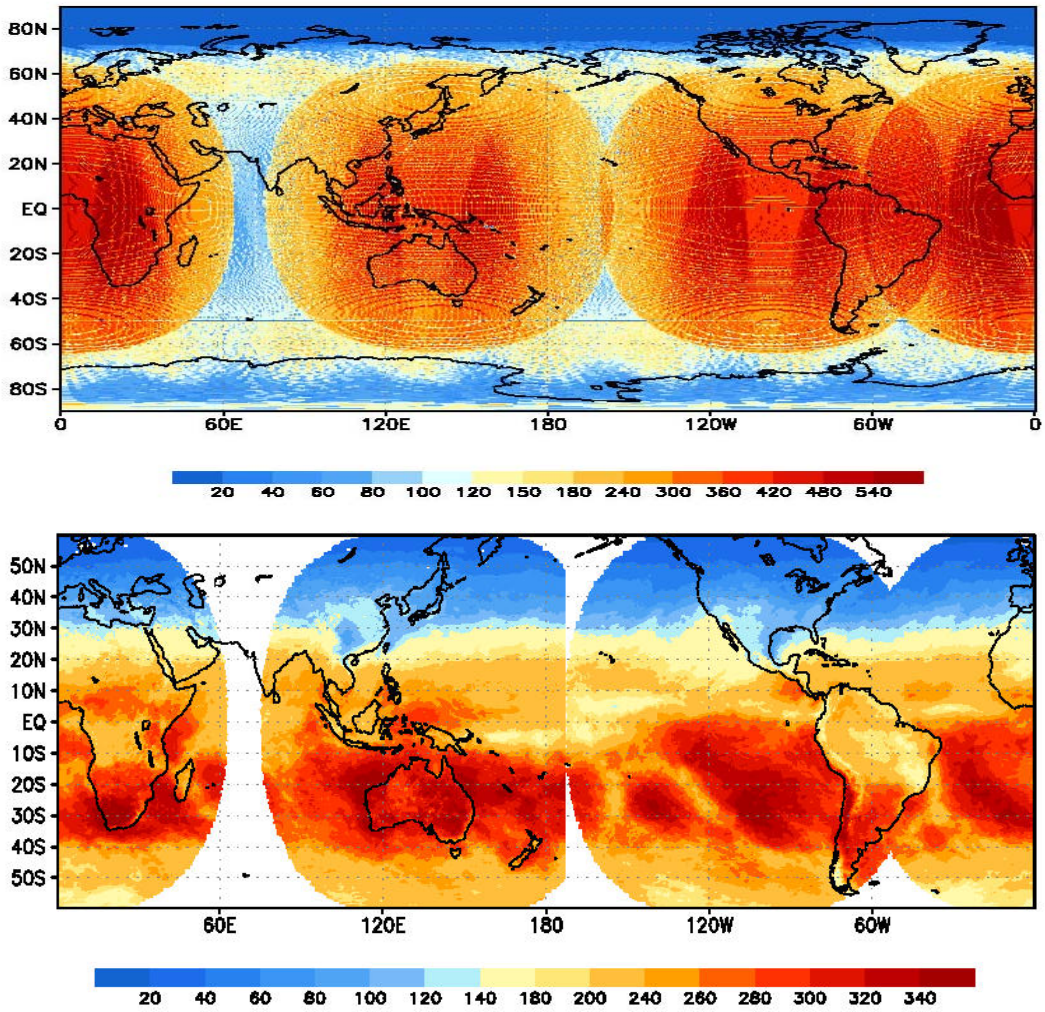

Figure 1. Upper: The frequency distribution of ISCCP geostationary and polar orbiting satellite observations at DX resolution for October 1986. Lower: Monthly mean shortwave downward flux (W/m^2) for January 1992 derived from GOES, METEOSAT, and GMS ISCCP DX data independently.

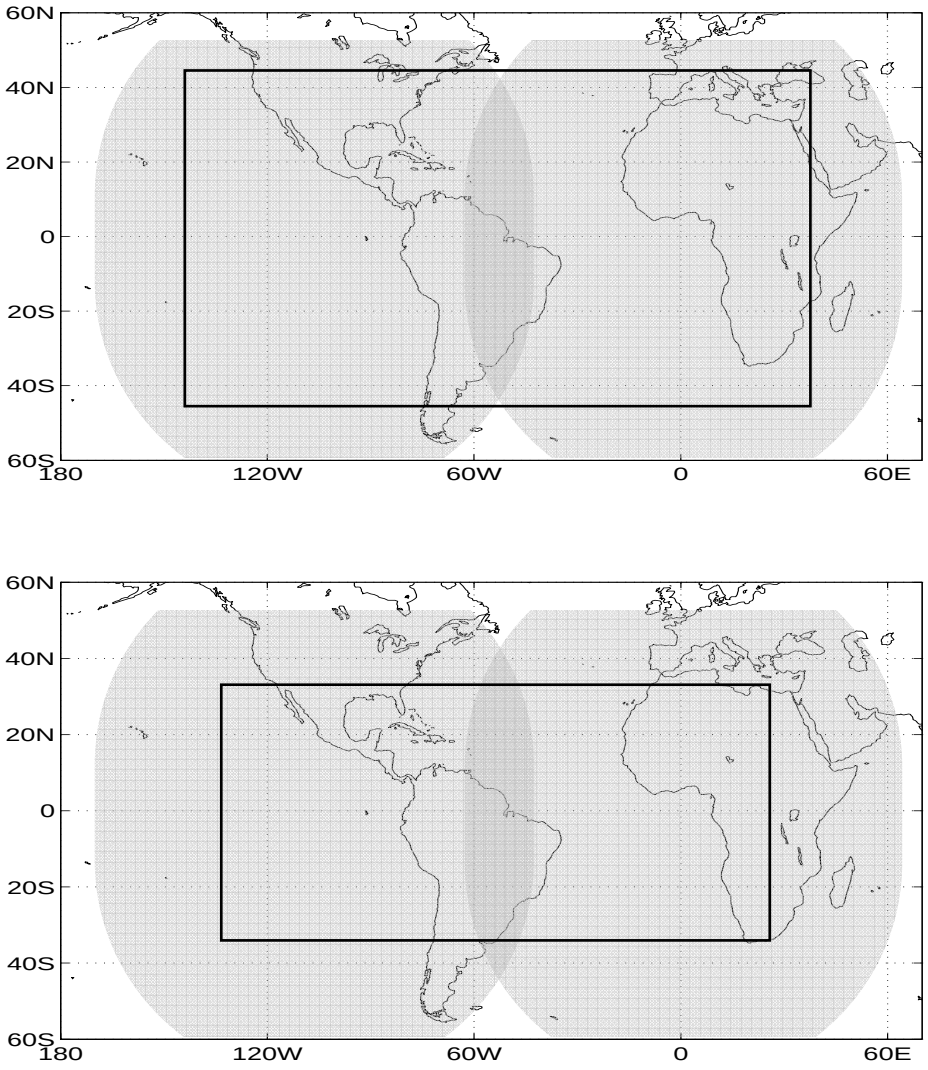

Figure 2. Illustration of two (top and bottom) possible ways to select anchor regions (rectangle in the middle) for EOF iteration. Inside rectangle: anchor region; outside rectangle: degraded region; hatched: overlap region; white: missing values. Upper: larger anchor region; Lower: smaller anchor region.

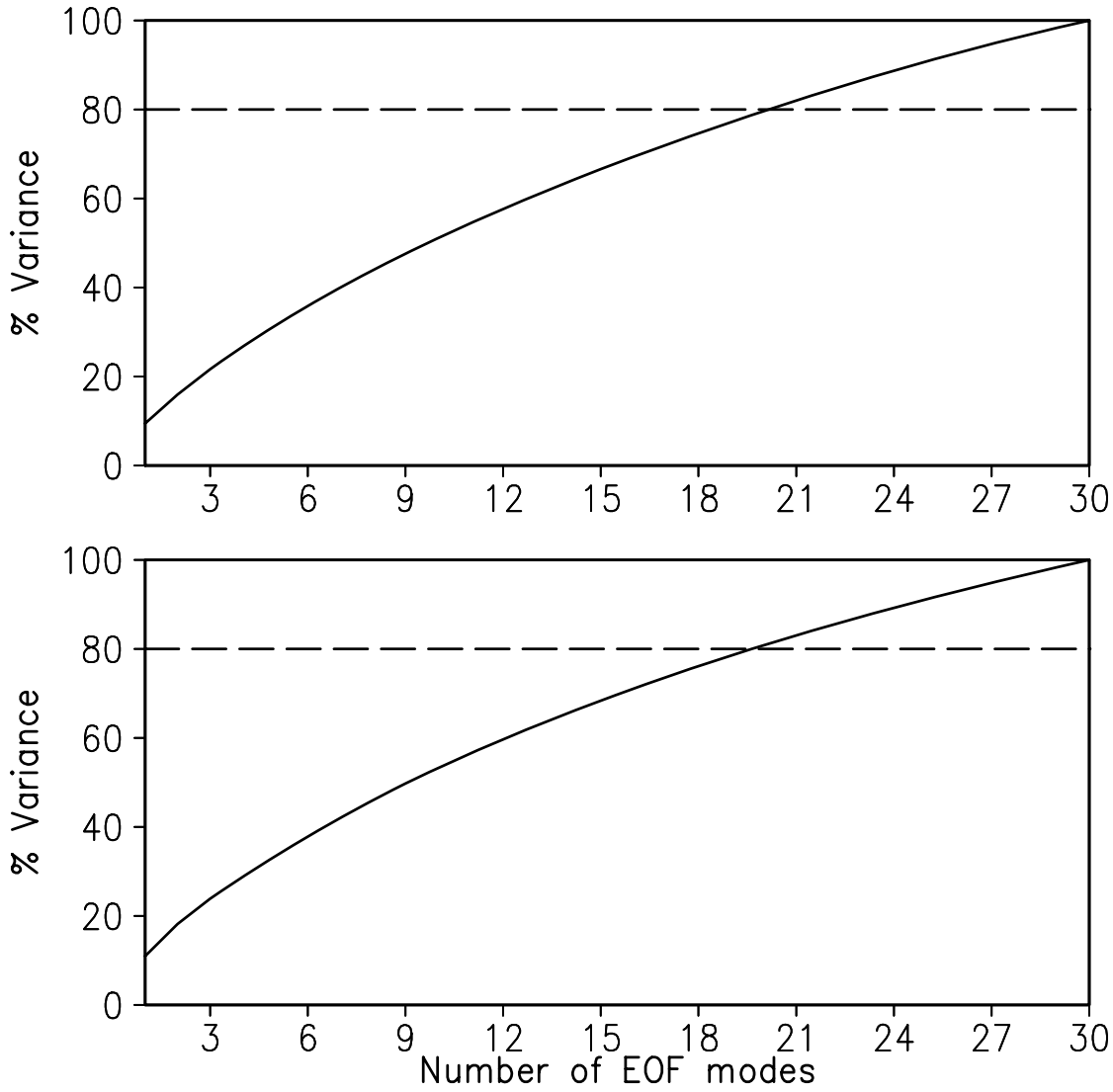

Figure 3. The explained % variance of shortwave surface fluxes by EOFs, as a function of the number of EOF modes used for January (top) and July (bottom) of 1992.

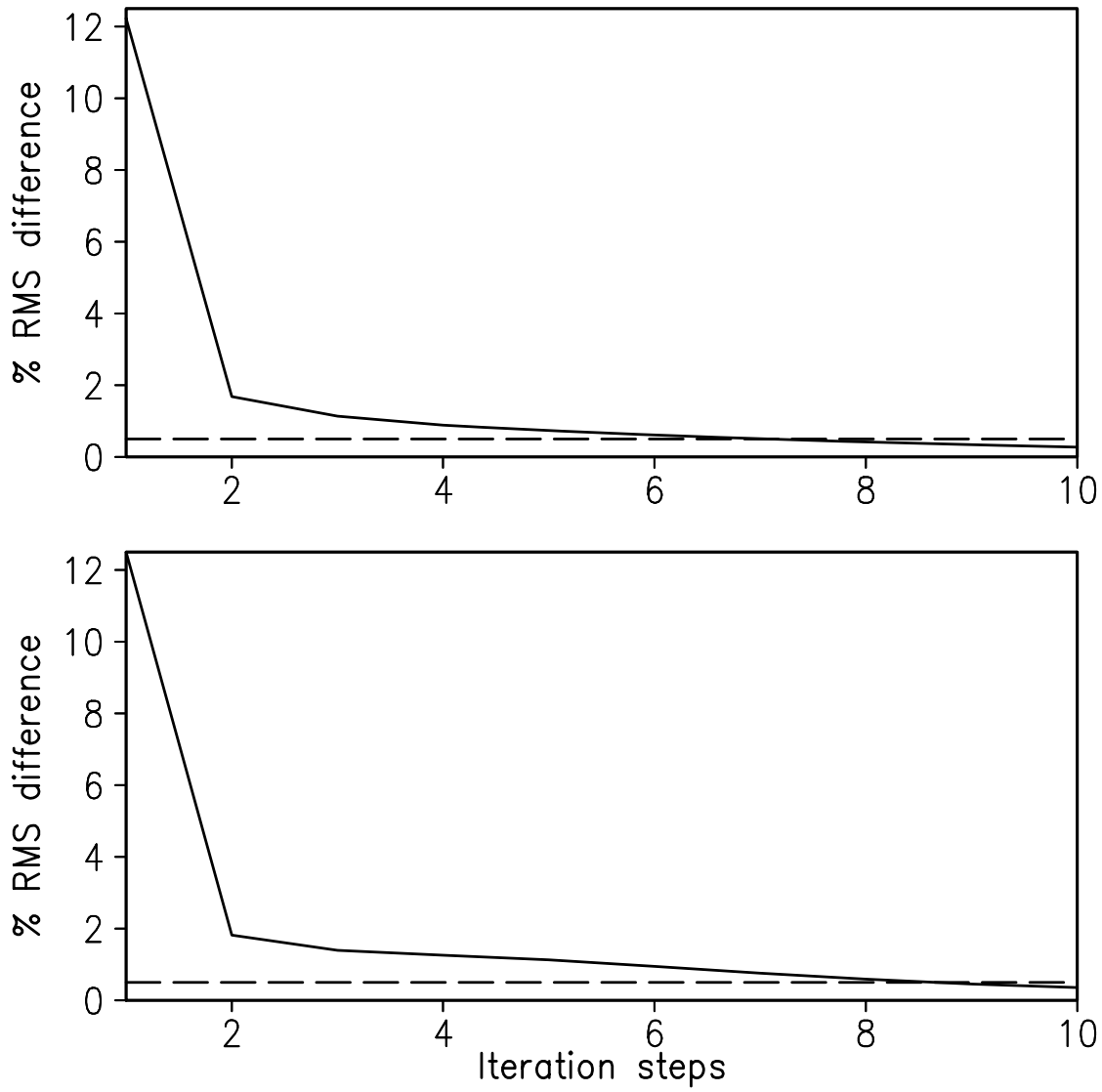

Figure 4. The RMS difference, normalized by the standard deviation, between successive iteration steps. When this difference becomes less than 0.5 %, the iteration process is stopped.

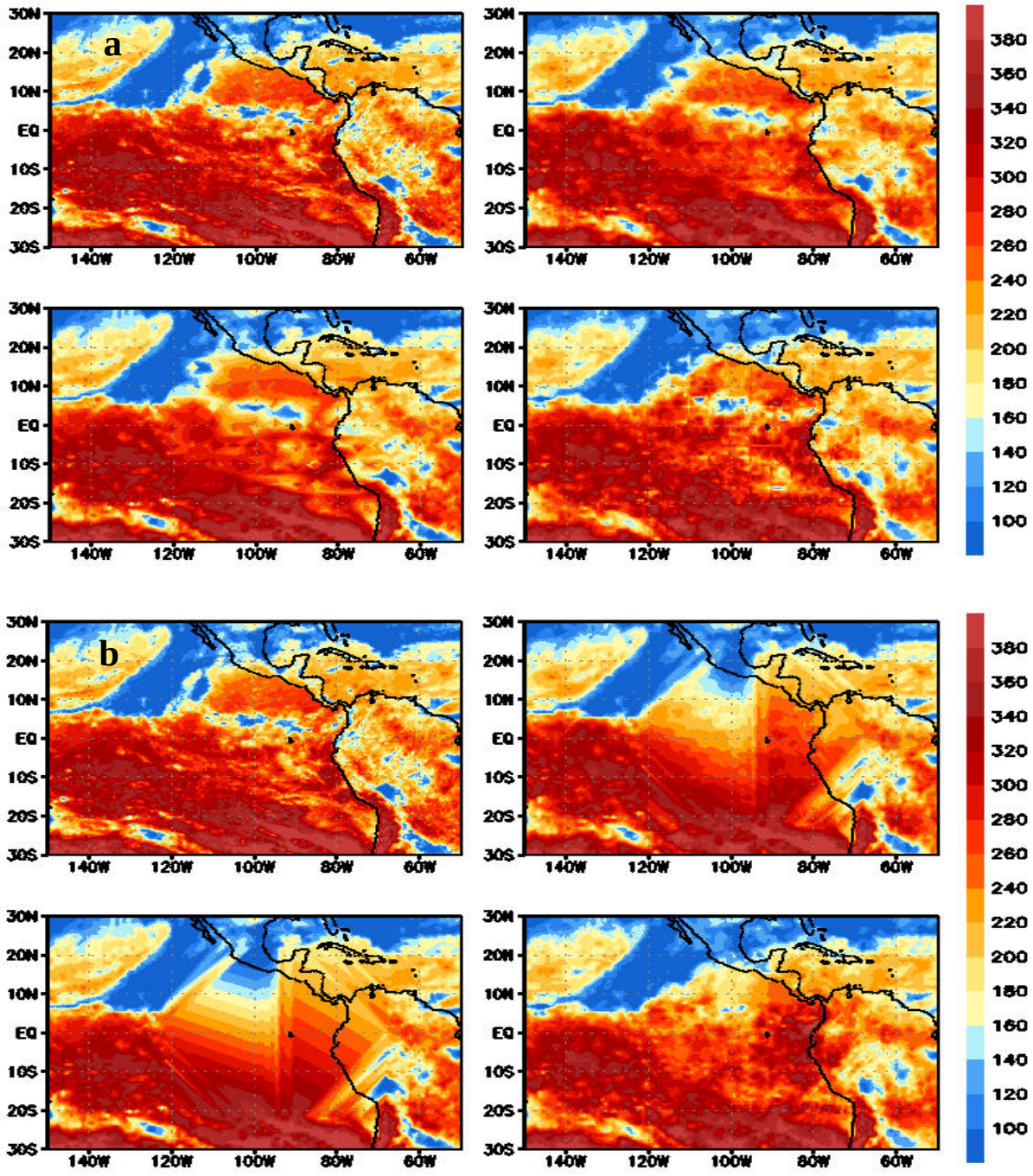

Figure 5. Upper four panels: The daily shortwave downward fluxes over region for control test 1 on January 2, 1992 from actual observations (upper left panel), estimated by Renka interpolation scheme (lower left panel), Smith's EOF reconstruction scheme (upper right panel), and EOF iteration scheme (lower right panel). Lower four panels: Same as upper but for control tests 2.

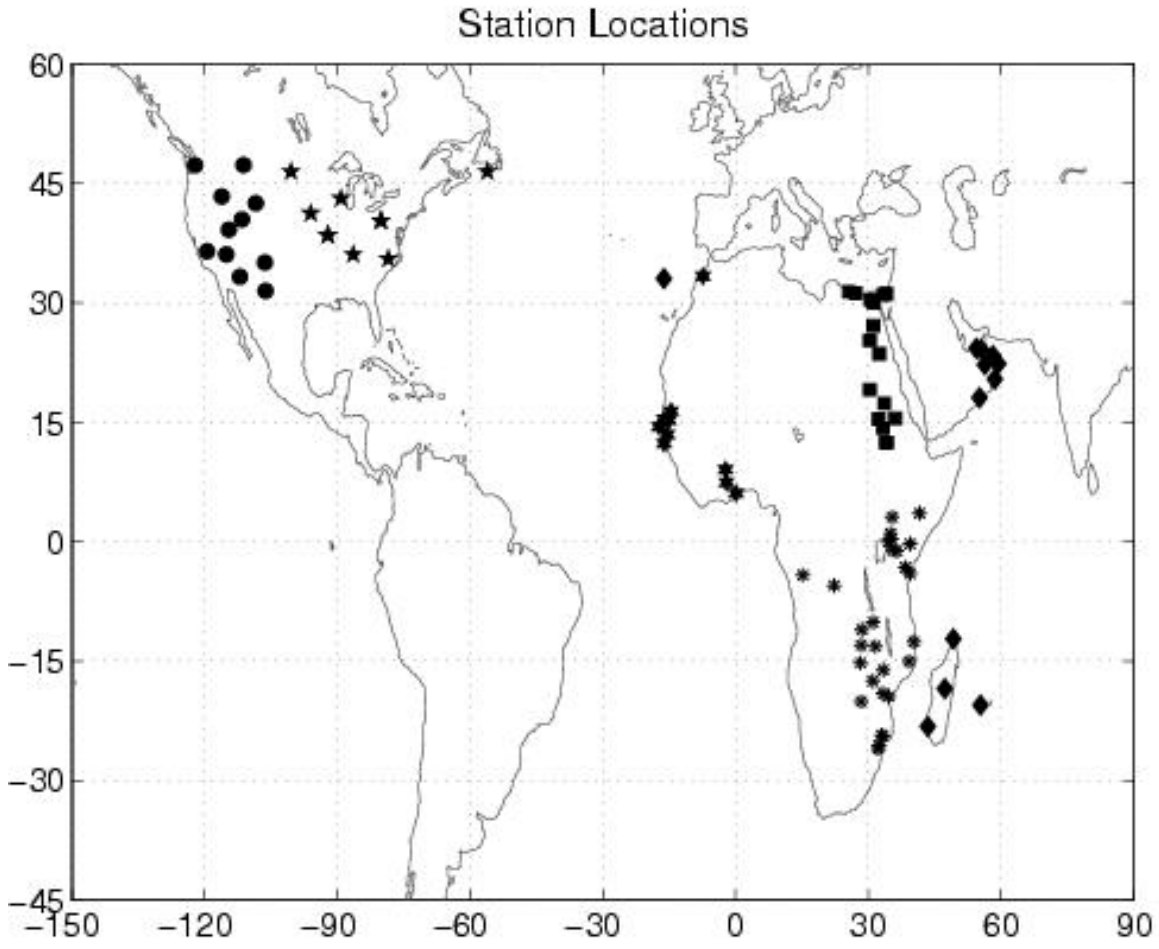

Figure 6. Location of stations used for evaluation of the improvements in surface radiative fluxes as a result of the proposed merging procedure. Circle: North America Region 1 (NA1); oentagram: North America Region 2 (NA2); hexagram: Africa Region 1 (AF1); asterick: Africa Region 2 (AF2); square: Africa Region 3 (AF3); and diamond: Africa Region 4 (AF4).

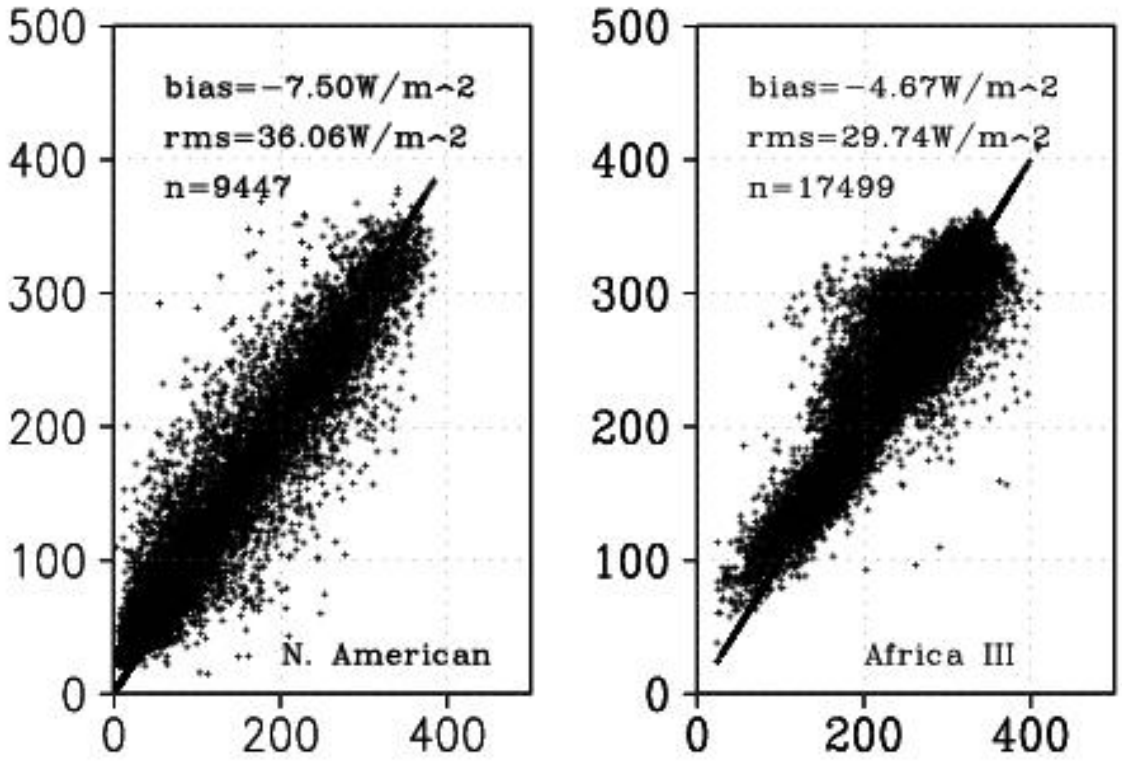

Figure 7. Comparison of merged surface SW radiative fluxes as derived from ISCCP DX data gridded to 0.5^0 against ground observations for the period 1989-1993. Over North America, results are illustrated for all available stations. Over Africa, results are illustrated only for stations in region III.

Table 1. Evaluation of the Ranka, Smith and the EOF merging scheme using ground observations of radiative fluxes. Given are the bias numbers (first) and the rms (second). When all observations over N. America and Africa were used, two experiments were performed: a) using all data; b) using data from areas where no satellite observations were available and the satellite values used are the result of the EOF fusing method.

Regions	**Ranka Interpolation**		**Smith Method**		**EOF Merging**	
	All data	Missing Data	All data	Missing Data	All data	Missing Data
N America	-8.41/38.83	-12.06/52.66	-8.08/38.84	-6.62/52.52	-7.50/36.06	-6.61/48.83
Africa	-13.29/44.83	-45.07/69.68	-10.63/41.73	-43.53/61.73	-10.65/40.96	-43.50/61.62
N America I	-5.32/37.67		-5.62/36.99		-4.88/35.56	
N America II	-11.56/37.41		-10.90/37.50		-10.16/33.56	
Africa I	-22.35/43.18		-20.42/41.17		-20.42/40.27	
Africa II	-1.77/42.81		-0.99/40.91		-0.99/39.71	
Africa III	-7.29/33.07		-4.64/30.15		-4.67/29.74	
Africa IV	-19.57/45.97		-19.48/43.57		-19.53/43.29	